



# Spatial substrate heterogeneity limits microbial growth as revealed by the joint experimental quantification and modeling of carbon and heat fluxes

Martin-Georg Endress<sup>a,1,\*</sup>, Fatemeh Dehghani<sup>b,1</sup>, Sergey Blagodatsky<sup>a,c</sup>, Thomas Reitz<sup>b</sup>, Steffen Schlüter<sup>d</sup>, Evgenia Blagodatskaya<sup>b</sup>

<sup>a</sup> Institute of Zoology, University of Cologne, 50923, Cologne, Germany

<sup>b</sup> Department of Soil Ecology, Helmholtz Centre for Environmental Research – UFZ, 06120, Halle/Saale, Germany

<sup>c</sup> Institute of Meteorology and Climate Research, Department of Atmospheric Environmental Research (IMK-IFU), Karlsruhe Institute of Technology (KIT) – Campus Alpin, 82467, Garmisch-Partenkirchen, Germany

<sup>d</sup> Department of Soil System Science, Helmholtz Centre for Environmental Research – UFZ, 06120, Halle/Saale, Germany

## ARTICLE INFO

### Keywords:

Calorespirometry  
Nutrient limitation  
Oxygen limitation  
Carbon use efficiency  
Energy use efficiency  
Microbial-explicit modeling

## ABSTRACT

Spatial heterogeneity is a pervasive feature of soils, affecting the distribution of carbon sources as well as their microbial consumers. Heterogeneous addition of substrates typically results in delayed microbial growth compared to homogeneous addition, and this effect has frequently been attributed to spatial separation of microorganisms from their food. We investigated the importance of two other potential causes of this effect, the availability of nutrients and oxygen, by measuring heat and CO<sub>2</sub> release along with O<sub>2</sub> consumption from soil samples after homogeneous or heterogeneous addition of glucose as well as with or without further addition of a nutrient solution. We then employed a microbial-explicit model to quantitatively interpret our observations. The results revealed that delayed growth after spatially heterogeneous substrate addition was primarily caused by nutrient limitation. While sufficient co-location of all entities - substrate, microorganisms, and nutrients - is required for optimal growth, spatial separation of glucose and microorganisms only played a minor role in our experiment. Model simulations captured the dynamics based on aerobic growth and maintenance, utilizing a simple formulation of nutrient limitation coupled with dynamic transition of microbes between activity and dormancy. The model predicted an overall lower microbial activity over the course of the incubation in treatments with heterogeneous substrate addition. Despite reduced rates, neither the experimental carbon and energy balances nor modeling showed an effect of heterogeneity on the growth efficiency after 50 h of incubation. In all treatments, energy use efficiency exceeded carbon use efficiency by 9–21%. We found no evidence of anaerobiosis. The application of a bioenergetic framework facilitated the interpretation of complex experimental data and quantitatively captured the mechanisms underlying the effects of spatial heterogeneity.

## 1. Introduction

The fate of organic carbon (C) entering soil or stored as soil organic matter (SOM) is of critical importance to future climate change and to the provisioning of soil ecosystem services, and it is mediated in large part by soil microorganisms (Bardgett et al., 2008; Phillips and Nickerson, 2015; Crowther et al., 2019). The processes and factors controlling the decomposition and cycling of C and especially the fraction of consumed C that is used by microbes to form new biomass, often termed the microbial carbon use efficiency (CUE), have thus played a central

role in soil research for decades (Manzoni et al., 2018). Yet, the complexity and variability of natural soil environments that arises from the simultaneous occurrence of many physico-chemical (e.g., diffusion and sorption) and biological processes (e.g., diverse metabolic activity and microbial interactions) continue to challenge our understanding of microbial carbon cycling and especially CUE (Sinsabaugh et al., 2013; Geyer et al., 2016; Hagerty et al., 2018).

One important source of such challenges is the high degree of spatial and temporal heterogeneity in soils, both regarding the distribution of C substrates (e.g., Peth et al., 2014; Schlüter et al., 2022) as well as their

\* Corresponding author.

E-mail address: [m.endress@uni-koeln.de](mailto:m.endress@uni-koeln.de) (M.-G. Endress).

<sup>1</sup> Equal contributions.

potential microbial consumers (e.g., Raynaud and Nunan, 2014). Availability and input of C as well as suitable habitat in soils are necessarily patchy, e.g., concentrated in the rhizosphere or detritusphere, and the ecological relevance of this heterogeneity for microbial strategies and communities as well as for SOM persistence is well recognized (Kuzyakov and Blagodatskaya, 2015; Nunan, 2017; Lehmann et al., 2020). Multiple studies have evaluated the effect of substrate spatial heterogeneity on microbial C use by manipulating the substrate distribution experimentally. C derived from various compounds, ranging from labile C sources (Shi et al., 2021) to pesticides (Pinheiro et al., 2015), plant litter (Gaillard et al., 1999; Kandeler, 1999; Coppens et al., 2006; Magid et al., 2006; Poll et al., 2006; Védère et al., 2020) and plant-derived organic matter (Inagaki et al., 2023) has been used for this purpose. The role of spatial heterogeneity was also investigated by manipulating soil spatial structure (Strong et al., 2004; Juarez et al., 2013; Tian et al., 2015). The results of such experiments revealed pronounced effects of spatial heterogeneity, like a steep decline in activity with increasing distance from substrate hotspots, or a reduced and delayed activity in the case of heterogeneous substrate addition when compared to homogeneous addition (but see Juarez et al., 2013 and the subsoil results in Inagaki et al., 2023).

Mechanistically, several processes could explain these experimental observations. Granted that most soil microbes are expected to follow stationary sit-and-wait strategies (Nunan et al., 2020), the most frequently offered explanation invokes the spatial separation between microbial consumers and C sources. In this situation, the availability of assimilable substrate is mediated by the diffusion of monomers (either added directly or resulting from the decomposition of polymers) and enzymes (to decompose polymers, Or et al., 2007) as well as by physical C source accessibility (Dungait et al., 2012). Conceptually, a reduction and delay in activity in the case of heterogeneous substrate distribution may then result from a considerable portion of soil microbes that cannot access the substrate and remains C- and energy-limited. However, other limitations may also occur, especially under local excess of substrate. For example, low availability of essential nutrients like nitrogen (N) has the potential to limit the rate of anabolism and thus microbial growth even if sufficient C is present. Such imbalanced stoichiometry reduces CUE and alters SOM utilization in natural soils, for example due to N-mining (Manzoni et al., 2012; Chen et al., 2014; Manzoni, 2017; Chakrawal et al., 2022), and might lead to overflow respiration (Russell and Cook, 1995). Likewise, microbial growth can be impeded if the rate of energy acquisition through catabolism is limited by local O<sub>2</sub> availability in the soil. While this is very common under water-saturated conditions, the mechanism is also relevant at intermediate moisture levels, in particular in microsites with high microbial activity, where the demand-driven onset of anaerobiosis may lower the rate and efficiency of microbial carbon use (Loecke and Robertson, 2009; Schlüter et al., 2019; Kim et al., 2021; Lacroix et al., 2023).

These mechanisms, depending on local availability of substrate, nutrients, and oxygen, likely mediate the effect of substrate spatial heterogeneity to varying degrees *in situ*, but untangling their contributions in particular experimental settings is a challenging task.

Theoretical and modelling frameworks frequently used to interpret experiments (e.g., Korsaeath et al., 2001; Kuka et al., 2007; Moyano et al., 2013; Babey et al., 2017; Zech et al., 2022) recently turned towards leveraging the coupling between C and energy fluxes in soil as a new avenue to elucidate the microbial metabolism and specifically CUE and energy use efficiency (EUE) (e.g., Chakrawal et al., 2020; Bajracharya et al., 2022; Gunina and Kuzyakov, 2022; Wang and Kuzyakov, 2023). For example, several studies evaluated the calorespirometric ratio (CR, Hansen et al., 2004; Barros et al., 2016) of heat to CO<sub>2</sub> production during microbial growth in soil, both experimentally (e.g., Barros et al., 2010; Herrmann and Bölscher, 2015) and theoretically (Chakrawal et al., 2020, 2021, Endress et al., 2024). These efforts demonstrated the potential of the framework to, e.g., monitor changes in microbial CUE or to detect a switch to anaerobic metabolism, especially if CR observations

are supported by modelling efforts to disentangle and quantify these effects. However, this integration of experimental data with process-based bioenergetic models that include an explicit representation of microbial biomass and its dynamics is still at an early stage, a challenge that persists with regard to biogeochemical models more generally (Wieder et al., 2015; Marschmann et al., 2019).

In this study, we investigated the impact of substrate spatial heterogeneity on the dynamics and the efficiency of soil microbial growth from the perspective of coupled C and energy fluxes. To that end, we measured CO<sub>2</sub> and heat production after either homogeneous or heterogeneous addition of glucose as a labile C- and energy source. Based on similar studies, we hypothesized (i) that heterogeneous substrate application would result in lower and delayed microbial growth compared to a homogeneous treatment. To distinguish the potential limiting factors underlying such a pattern, we also monitored the consumption of O<sub>2</sub> throughout the incubations and factorially added nutrients along with glucose. Using this design, transitions to anaerobic pathways due to local O<sub>2</sub> deficiency can be detected both in the CR as well as in the direct O<sub>2</sub> measurements, while local nutrient depletion in hotspots with excess glucose would be alleviated in treatments where glucose is supplied in combination with additional nutrients. We further hypothesized (ii) that these mechanisms are more important causes of reduced microbial growth compared to the spatial availability of glucose itself. Finally, we combined our experimental findings with a simple microbial-explicit model including coupled C- and heat fluxes during growth on glucose to analyze and interpret our results in a quantitative framework, and to discern the degree to which growth limitation (e.g., by O<sub>2</sub> or nutrients) can be inferred from the C- and energy balance.

## 2. Materials and methods

### 2.1. Incubation setup

The soil used in this experiment is classified as a Haplic Luvisol and was sampled during September 2021 from the experimental site of Dikopshof, University of Bonn, Germany, established in 1904 (Holthusen et al., 2012; Seidel et al., 2021). Relevant characteristics of the soil are given in Table S1. The soil was sieved through a 2 mm mesh, air dried and stored at room temperature. It was then preincubated at a water content of 14% (w/w, 45.5% of water holding capacity, WHC) for 10 days before the start of the experiment. Water loss due to evaporation was compensated by regular water addition, and any seedlings growing during the preincubation were removed by hand.

Four treatments were considered to investigate the effect of substrate heterogeneity in soil. The soil samples were either amended with a solution of glucose in water or glucose in a nutrient solution ((NH<sub>4</sub>)<sub>2</sub>SO<sub>4</sub> 9.5 g/L, KH<sub>2</sub>PO<sub>4</sub> 14.75 g/L, MgSO<sub>4</sub>(H<sub>2</sub>O)<sub>7</sub> 19 g/L) at a rate of 1 mg glucose per g soil and with a C:N:P ratio of 10:1:1. In addition, application of glucose was either drop by drop on the soil surface without additional mixing, inducing a heterogeneous substrate distribution, or the soil was manually well mixed after substrate amendment. The added solutions brought the final soil water content to 16% (w/w, 52 % WHC).

### 2.2. Calorimetry and respirometry measurement

CO<sub>2</sub> efflux after substrate addition was monitored using a Respirometer (Respicond V, Sweden) in which 25.8 g (DW) of soil were incubated in 280 ml vessels that were kept in a water bath at a constant temperature of 20 °C. CO<sub>2</sub> release rate (mg CO<sub>2</sub> h<sup>-1</sup>) was quantified via the decrease in the conductance of a KOH solution (10 ml, 0.6 M) in the vessels (Chapman, 1971; Nordgren, 1988). Heat release was measured from 3.88 g (DW) soil incubated in 20 ml glass ampoules using an isothermal calorimeter (TAM Air, TA Instruments, Germany) at the same constant temperature of 20 °C. A comparable soil height of 0.9 cm as well as a minimum headspace to soil ratio of 4 was used in both the Respirometer vessels and TAM Air ampoules. The vessels used for the

incubations are shown in Fig. S1.

### 2.3. O<sub>2</sub> measurement

In a parallel setup, we measured O<sub>2</sub> consumption via needle-type O<sub>2</sub> microsensors (NFSG-PSt1, PreSens Precision Sensing GmbH, Regensburg, Germany) that were placed in the headspace of 20 ml glass ampoules with the same experimental setup as used for the TAM Air measurements. O<sub>2</sub> saturation (%; 100% = 21.22 kPa) was monitored every 15 min.

### 2.4. Microbial biomass quantification and determination of residual glucose

Additional incubations were carried out for well-mixed samples with only glucose addition (i.e., without nutrient addition) for the determination of microbial biomass production via an increase in double-stranded DNA (dsDNA) as well as quantification of the residual amount of glucose. Again, these incubations were carried out in 20 ml ampoules ensuring the same experimental setup as used for the TAM Air measurements. 300 mg of fresh soil was sampled destructively at several time points (0, 18, 21, 25, and 47 h after substrate addition). The dsDNA in the soil was extracted using the PowerSoil DNA isolation kit (QIAGEN, Germany) with small modifications in the protocol by performing an additional physical cell lysis using a homogenizer (Precelleys-24, PEQ-LAB, Germany) in three batches each for 45 s at 5000 rpm. DNA quantification was done by a NanoDrop ND-8000 spectrophotometer (Thermo Fisher Scientific, Dreieich, Germany). An increase in the microbial biomass was related to changes in the DNA by a conversion factor of  $f_{DNA} = 16.5$  calculated as (Zheng et al., 2019):

$$f_{DNA} = \frac{MBC_i}{DNA_i} \quad (\text{Eqn. 1})$$

Here,  $MBC_i$  is the initial amount of soil microbial biomass carbon (MBC) as determined by chloroform fumigation extraction (155  $\mu\text{g C g}^{-1}$  soil, details in S1 Text), and  $DNA_i$  is the initial dsDNA content of the soil (9.4  $\mu\text{g DNA g}^{-1}$ ). For the quantification of residual glucose, 200 mg of soil (DW), taken at 0, 3, 6, 21, 23, and 24 h after glucose addition to the soil, was dispersed in 30 ml of DI water followed by shaking on a rotary shaker at room temperature for 30 min. Afterwards, the suspension was centrifuged at 4000 rpm for 10 min. Thereafter, 20 ml of supernatant was transferred to determine residual glucose by a glucose colorimetric/fluorometric assay kit MAK263 (Sigma-Aldrich, Germany) in which glucose is oxidized to generate a fluorometric product, proportional to the glucose amount. Glucose quantification was performed based on the manufacturer's protocol.

CO<sub>2</sub> measurements were performed with 4 replicates, all other experiments were performed in triplicate. All process rates (CO<sub>2</sub> and heat production, O<sub>2</sub> consumption) were corrected by subtracting the average rates of unamended (control) incubations, which were also performed in triplicate.

### 2.5. Calculations and statistics

**Analysis of CO<sub>2</sub> and heat production.** Maximum rates of CO<sub>2</sub> and heat release as well as their corresponding time points were determined from the time series of all replicates. For heat release, maximum rates and time points could be identified unambiguously from the raw time series. For CO<sub>2</sub> and O<sub>2</sub>, we applied a moving average with a window width of 2 h to the time series prior to determination of maximum rates and time points to enable unambiguous identification. The results were tested for the effects of substrate heterogeneity and nutrient addition using a two-way ANOVA with contrasts between treatments at a significance level  $\alpha = 0.05$  as implemented in the emmeans package (v. 1.8.9, Lenth, 2023) in R (v. 4.3.2, R Core Team, 2023).

**Cumulative and dynamic ratios.** The cumulative ratios of heat to CO<sub>2</sub> production (CR), heat production to O<sub>2</sub> consumption (CR<sub>O<sub>2</sub></sub>) and CO<sub>2</sub> production to O<sub>2</sub> consumption (respiratory quotient, RQ) were calculated using the respective mean cumulative values after 50 h of incubation time. Standard deviations were estimated via error propagation of the standard deviations of the constituting variables (S1 Text). Due to initial disturbance in the Respicond and the calorimeter, the first 2.5 h were discarded for the cumulative analysis (but raw data are provided in S1 Data). The effects of substrate heterogeneity and nutrient addition were tested using an approximate permutation test for pairwise differences (van den Broek, 2012) with 10000 bootstrap iterations (details in S1 Text).

The dynamic ratios were calculated hourly from the corresponding rate data (mean of replicates). To mitigate the fluctuations caused by the high temporal resolution, the rates were smoothed using a moving average with a width of 4 h prior to calculating ratios. Due to the high sensitivity of the dynamic ratio to even small perturbations, it was calculated in the interval between 5 h and 50 h of incubation time to avoid artifacts caused by initial disturbance.

**CUE and EUE.** Apparent carbon and energy use efficiency was estimated from the cumulative release of CO<sub>2</sub> and heat, respectively, after 50 h of incubation time, i.e.,

$$CUE_s = 1 - \frac{C_{CO_2}}{C_{Glu}}$$

$$EUE_s = 1 - \frac{Q}{\Delta E_{Glu}}$$

Here,  $C_{CO_2}$  and  $Q$  denote the mean cumulative CO<sub>2</sub> and heat produced per gram of soil after 50 h, respectively, whereas  $C_{Glu}$  and  $\Delta E_{Glu}$  denote the initial amount of carbon and energy added as glucose per gram of soil. We use the subscript  $s$  for CUE and EUE to denote the substrate-based nature of these estimates (Hagerty et al., 2018) and emphasize that these rely on the assumption of complete substrate consumption at the time of calculation (Wang and Kuzyakov, 2023). Again, the effects of substrate spatial heterogeneity and nutrient addition were tested using a two-way ANOVA with contrasts.

**O<sub>2</sub> consumption.** O<sub>2</sub> saturation  $O_{sat}$  [%] was converted to mol per gram soil (DW) via the ideal gas law according to

$$O_2 \left[ \frac{\text{mol}}{\text{g}} \right] = \frac{O_{sat}}{100} O_{am} \cdot \frac{V}{T \cdot R} \cdot \frac{1}{W}$$

where  $O_{am} = 21.22$  [kPa] denotes the atmospheric oxygen partial pressure,  $V = 0.019$  [l] is the estimated volume of air in the ampoule,  $T = 293.15$  [K] is experimental temperature,  $R = 8.314$  [J/(mol\*K)] is the gas constant, and  $W = 3.88$  [g] is the dry weight of the soil sample (DW).

### 2.6. Modeling

We use a modified version of the ordinary differential equation (ODE) model presented in (Endress et al., 2024) to quantitatively simulate the coupled carbon and energy fluxes during microbial growth on glucose in soil. In contrast to the original formulation, the model only includes aerobic metabolism, but considers an additional nutrient limitation.

The model structure (Fig. 1) includes three carbon pools: biomass  $X$ , glucose  $S$ , and CO<sub>2</sub>, similar to the complex physiological model used in Chakrawal et al. (2021). It represents the microbial utilization of added glucose following Monod kinetics (at rate  $U$ ) for aerobic growth, as well as maintenance respiration, fueled first by glucose (exogenous maintenance,  $M_S$ ) and later by biomass consumption (endogenous maintenance,  $M_X$ , see Wang and Post, 2012). In addition, the model also accounts for changes in microbial activity via the index of physiological state  $r$  (Panikov, 1996; Blagodatsky and Richter, 1998), which partitions the biomass into an active, growing fraction  $rX$  as well as a dormant

fraction  $(1-r)X$  that only performs maintenance, depending on substrate availability. Finally, we also model nutrient limitation by including an additional unspecified nutrient pool  $N$ , which acts as an additional essential component for the anabolic reaction and also follows Michaelis-Menten kinetics (i.e., the growth kinetics  $U$  now depend on two substrates, carbon  $S$  and nutrient  $N$ , Zimm et al., 2004). In contrast to glucose, which is added in batch at time 0, the model nutrient concentration gradually replenishes at a rate  $I(N_0-N)$  proportional to the degree of nutrient depletion, thus mimicking diffusive (re-)supply from the surrounding soil.

To investigate the potential impact of a delayed  $CO_2$  detection due to diffusion of  $CO_2$  from the soil to the KOH solution, we also implemented a model variant with an additional carbon pool representing the concentration of  $CO_2$ -C accumulating in the KOH solution ( $C_{Alkali}$ ). This pool is characterized by slightly delayed dynamics due to the additional transport process, and it is utilized for all subsequent analyses of the modified model instead of the (soil)  $CO_2$  pool that is used in the standard model.

All model ODEs were implemented in Python (version 3.9.18) and simulations were obtained via numerical integration using the 'Radau' method of the *solve\_ivp* function in the *Scipy* package (Virtanen et al., 2020). Initial biomass and glucose concentrations were set to the experimental values, whereas initial cumulative heat and  $CO_2$  were set to 0. The initial nutrient concentration as well as the initial active fraction of microbes were treated as free parameters. The model was calibrated against the measured rates of heat and  $CO_2$  release of the individual treatments, i.e., we obtained 4 sets of optimized parameter values corresponding to the combinations of substrate spatial heterogeneity (homogeneous, heterogeneous) and nutrient addition (with, without). Parameter optimization was done using the Levenberg-Marquardt algorithm in the *minimize* function of the *lmfit* package (Newville et al., 2023) with upper and lower bounds on individual parameters.

The detailed model formulation and rationale as well as an in-depth description of the numerical procedures are provided in the supplementary materials and methods (S1 Text). A list of all variables and parameters including their units is provided in Table S2.

### 3. Results

#### 3.1. $CO_2$ and heat release and $O_2$ consumption

The rates of  $CO_2$  and heat release as well as  $O_2$  consumption showed a broadly consistent pattern indicating substantial microbial growth

after batch glucose input in all treatments, with a distinct maximum after 20–25 h (Fig. 2). However, both the mode of glucose application and the addition of nutrients had characteristic and interacting effects on the observed dynamics.

In treatments without nutrient addition, heterogeneous application of glucose resulted in significantly lower maximum rates of carbon and heat release (Fig. 2 a, c), which reached only 50–55% of the maximum values observed after homogeneous glucose application (ANOVA results in S1 Data). On the other hand, both  $CO_2$  and heat continued to be released at elevated rates in these incubations over the full 50 h duration, whereas they returned to near-basal levels within that time span in samples with homogeneous glucose addition (Fig. 2a–c). While less pronounced, these characteristics were also present in the measured rates of  $O_2$  consumption (Fig. 2e). Headspace  $O_2$  concentrations remained oxalic throughout the experiment in all treatments (Fig. S2).

In contrast, such effects of heterogeneous substrate application were strongly reduced in treatments with nutrient addition. Maximum rates of  $CO_2$  and heat release as well as  $O_2$  consumption were similar or only slightly lower in heterogeneous treatments when compared to homogeneous ones, and all rates also decreased to similar levels within 50 h (Fig. 2b–d,f). Nonetheless, maximum values in incubations with heterogeneous glucose application were reached slightly later (~2 h) than in those with homogeneous application. While this effect was only significant for heat, it was entirely absent in the treatments without nutrient addition (ANOVA results in S1 Data).

Thus, the effect of heterogeneous substrate application was most pronounced in samples without added nutrients. At the same time, nutrient addition altered the observed dynamics only in the case of heterogeneous substrate application, with barely any discernible impact in samples with homogeneous application.

#### 3.2. Cumulative calorimetric ratios and respiratory quotient

The ratios of cumulative heat release to  $CO_2$  release as well as to  $O_2$  consumption (CR and  $CR_{O_2}$ , respectively) showed similar values with no significant differences across treatments. The same was true for the respiratory quotient (RQ) of  $CO_2$  release to  $O_2$  consumption. Hence, from a cumulative perspective, neither the mode of substrate application nor the addition of nutrients had a significant effect (Fig. 3).

Furthermore, no ratio indicated any substantial deviation from values expected for aerobic metabolism in our incubation after 50 h. Specifically, the observed average CR values of 344–403 kJ/mol C agree with predictions for efficient aerobic growth on glucose, which lie in the range of ~250–469 kJ/mol C (Barros et al., 2010). Similarly, average

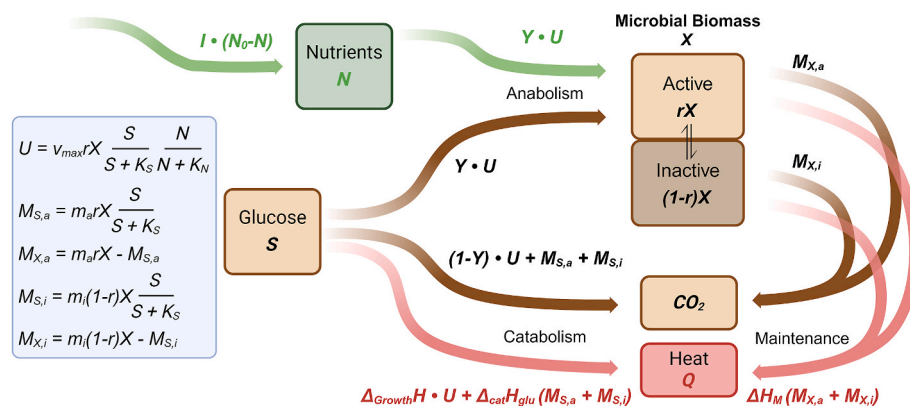


**Fig. 1.** Dynamic model structure representing aerobic microbial growth after glucose addition to soil. Microbial biomass  $X$  is initially in a largely inactive state (fraction  $1-r$ ), but quickly becomes active (fraction  $r$ ) in the presence of substrate  $S$ . This substrate is consumed following Michaelis-Menten kinetics at a rate  $U$  and partitioned between anabolic and catabolic pathways according to a growth yield coefficient  $Y$ . The uptake rate is further co-limited by the availability of a proxy nutrient pool  $N$  required for anabolism. Moreover, both active and inactive biomass produce additional  $CO_2$  and heat via exogenous maintenance ( $M_S$ , fueled by glucose consumption) and endogenous maintenance ( $M_X$ , fueled by biomass consumption). The total modelled  $CO_2$  and heat production is used to calibrate the model against experimental observations for each treatment. A detailed model description is provided in S1 Text.

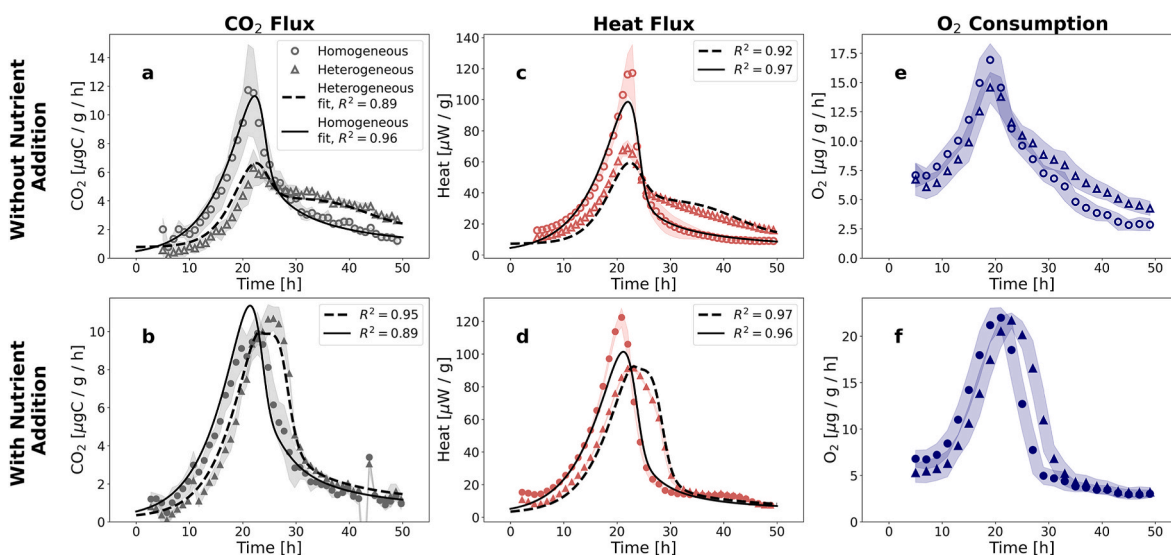


**Fig. 2.** Experimental observations (mean  $\pm$  SD) and model simulations of CO<sub>2</sub> production (a, b,  $n = 4$ ), heat production (c, d,  $n = 3$ ) production and O<sub>2</sub> consumption (e, f,  $n = 3$ ) in soil after glucose amendment. The top row shows results obtained without nutrient addition (open symbols), while the bottom row shows results with addition of NPK solution (filled symbols). In both cases, rates of CO<sub>2</sub> and heat production as well as O<sub>2</sub> consumption differed markedly between homogeneous (circles) and heterogeneous (triangles) addition of glucose to the soil.

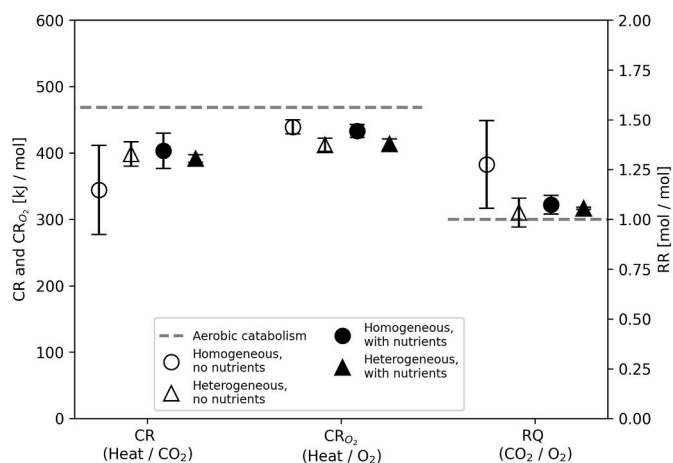


**Fig. 3.** Experimental ratios (mean  $\pm$  SD) calculated from cumulative CO<sub>2</sub> production, heat production and O<sub>2</sub> consumption after 50 h of incubation time. Open symbols indicate incubations without nutrient addition, filled symbols indicate incubations with NPK addition. Circles indicate homogeneous addition of glucose; triangles indicate heterogeneous addition. Dashed lines indicate the theoretical predictions for the corresponding ratios for the case of aerobic glucose catabolism.

CR<sub>O<sub>2</sub></sub> varied between 411 and 439 kJ/mol O<sub>2</sub>, while anaerobic heat contributions would elevate this ratio above the theoretical prediction of 469 kJ/mol O<sub>2</sub> (enthalpy of combustion of glucose, Hansen et al., 2004). Finally, the average RQ in all treatments was not significantly different from 1, which is the expected value for the aerobic decomposition of carbohydrates.

### 3.3. CUE and EUE

Both CUE<sub>S</sub> and EUE<sub>S</sub> based on cumulative CO<sub>2</sub> and heat release after 50 h indicated efficient aerobic growth with an average growth yield of 0.56–0.63 (carbon-based) and 0.65–0.68 (energy-based) across treatments (Fig. 4a). Generally, EUE was slightly higher than CUE in all incubations (i.e., observations are above the dotted line in Fig. 4a), and their relationship was in line with the theoretical expectation for aerobic

growth on glucose (dashed and solid lines in Fig. 4a, details in S1 Text). Moreover, the observed relationship between CUE<sub>S</sub> and CR also was broadly consistent with theory (Fig. 4b), although the quantitative prediction depends on the assumed composition of microbial biomass as summarized by its degree of reduction,  $\gamma_B$  (which is controlled by the C: N ratio of biomass, see Hansen et al., 2004; Chakrawal et al., 2020; Yang et al., 2024 and S1 Text). However, both CUE<sub>S</sub> and CR showed substantial variability, in particular for the treatment with homogeneous glucose application and no nutrient addition, which was characterized by larger deviations in the CO<sub>2</sub> release rate between replicates (Fig. 2a).

Overall, neither the mode of substrate application nor the addition of nutrients significantly affected CUE<sub>S</sub>, while nutrient addition slightly reduced EUE<sub>S</sub> irrespective of the mode of substrate application (ANOVA results in S1 Data).

### 3.4. Model behavior and performance

The dynamic model achieved good fits to the experimental observations in all treatments (Fig. 2 a-d,  $R^2 = 0.89$ – $0.97$ ) and adequately represented the general dynamics of CO<sub>2</sub> and heat release over the 50 h after addition of glucose. In particular, the model captured the prolonged release of CO<sub>2</sub> and heat in the case of heterogeneous substrate application without nutrient addition (Fig. 2 a, c) via its simple representation of nutrient dynamics.

The model also achieves a very good correspondence with experimental measurements of remaining glucose over time in the one treatment where this data is available (Fig. S3a). There was also a broad agreement between the predicted microbial biomass growth in the model and that inferred from dsDNA, although the relative biomass increase in the model (2.45-fold after 50h) exceeded the relative increase in dsDNA in the same treatment (which increased 1.84-fold, Fig. S3b, details in S1 Text).

The calibration results for all parameters and treatments along with uncertainty estimates are provided in S1 Data. Generally, the optimized values of most parameters were well comparable for all treatments and showed a plausible range and pattern (e.g., high aerobic yield coefficients and higher maintenance costs for the active fraction than in the inactive fraction, calibration results in S1 Data). However, the parameters controlling the activity state of the microbial population differed between treatments with homogeneous and heterogeneous glucose

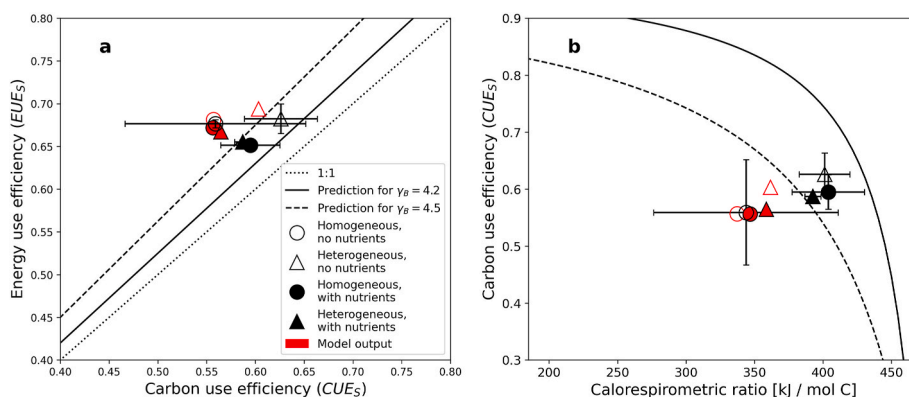


**Fig. 4.** Estimates of CUE, EUE and CR (mean  $\pm$  SD) based on cumulative CO<sub>2</sub> and heat production after 50 h of incubation. Black symbols are based on experimental observations, red symbols were obtained from corresponding model simulations. The solid and dashed lines show the theoretical CUE-CR relationships for aerobic growth on glucose assuming a biomass degree of reduction ( $\gamma_B$ ) corresponding to C:N ratios of 5 ( $\gamma_B = 4.2$ ) and 10 ( $\gamma_B = 4.5$ ), respectively (Yang et al., 2024). Symbol styles correspond to Fig. 3 a EUE<sub>s</sub> and CUE<sub>s</sub> were comparable across treatments and are in line with theoretical predictions. b Relationship between estimated CUE<sub>s</sub> and CR.

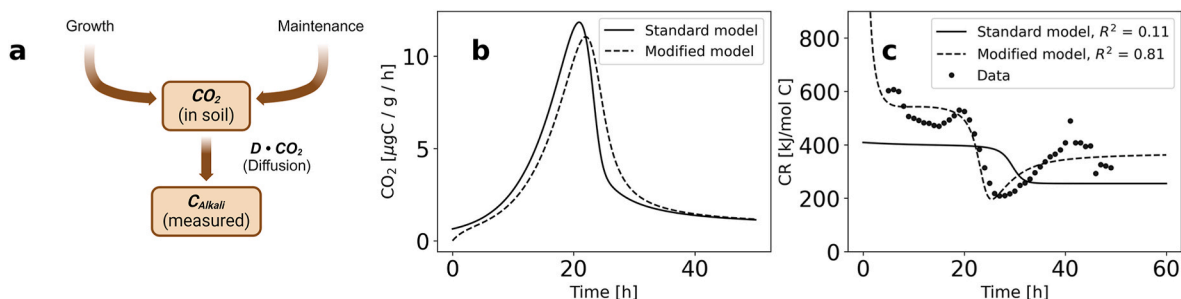


**Fig. 5.** Potential time delay between the production of CO<sub>2</sub> by microbes in the soil and its experimental detection in the alkali solution complicate the evaluation of dynamic CR. a In a modified model variant, CO<sub>2</sub> diffuses to the site of detection (e.g., alkali solution), where it accumulates in an additional pool ( $C_{Alkali}$ ). b In the modified model, the measured rate of CO<sub>2</sub> release (i.e.,  $C_{Alkali}$ ) is systematically delayed compared to the standard model, which assumes instantaneous detection after production by microbes in the soil. c If CR is calculated from the ratio of the rates of heat and (measured) CO<sub>2</sub> release, the systematic delay of CO<sub>2</sub> in the modified model induces a temporal pattern that is qualitatively similar to those observed in experimental data (shown are the results for homogeneous glucose application and with nutrient addition, all curves and fits are shown in Fig. S4).

application. Specifically, the model predicted a lower initial active fraction of microbes as well as an overall lower activity over the course of the whole incubation in treatments with heterogeneous substrate application (Fig. S3c), regardless of nutrient addition. In terms of model calibration, this difference is tied to the overall slower dynamics in those treatments (see 3.1), and it can be intuitively thought of as a smaller fraction of the biomass being exposed (and reacting) to the available glucose, as expected in the case of heterogeneous application.

In terms of CR, the (purely aerobic) growth reaction used in the model corresponds to the solid line in Fig. 4b. However, the actual relationship between model CUE<sub>s</sub> and CR is altered by the maintenance metabolism (details in S1 Text) and broadly resembled experimental observations after calibration. Nonetheless, model CR tended to be lower than observations in all treatments other than the incubations with homogeneous substrate application and no nutrient addition, indicating that the final calibration slightly overestimated cumulative CO<sub>2</sub> release compared to cumulative heat release in those treatments (Figs. 2 and 4b).

### 3.5. Dynamic CR and model variant with delayed CO<sub>2</sub> detection

The dynamic CR calculated from the rates of heat and CO<sub>2</sub> production showed strong temporal variation in all treatments, including values well above and below those expected for simple aerobic growth (Fig. S4). Specifically, rate-based CR was high early in the incubation followed by a drop after the time of peak activity during the retardation

phase, and while this general pattern was observed for all treatments, it was more pronounced in the case of heterogeneous substrate addition (Figs. S4c and d).

Although the dynamic model captured such a qualitative shift from high to low CR, it did not reproduce the quantitative details, especially the very high values during the exponential growth phase (Fig. S4). However, the introduction of a moderate delay of the measured CO<sub>2</sub> release rate in the modified model improved the CR representation considerably (Fig. 5). In particular, the model delay of 1.2–1.8 h due to diffusion of CO<sub>2</sub> from the site of production in the soil to the site of detection in the KOH solution (Fig. 5a and b) resulted in a pronounced and characteristic pattern in the dynamic model CR similar to observations (Fig. 5c). While the model fit to the rate data improved only slightly across treatments compared to the standard model ( $R^2 = 0.93$ – $0.99$  instead of  $0.89$ – $0.97$ ), this difference was much more pronounced in the CR, where small changes in modelled rates induced large changes in modelled CR due to its nature as quotient (with  $R^2$  improving from  $-0.09$ – $0.81$  to  $0.27$ – $0.81$ , Fig. S4).

## 4. Discussion

### 4.1. Substrate spatial heterogeneity induces nutrient limitation of microbial growth

We observed marked differences in the dynamics of CO<sub>2</sub> and heat release from an arable soil after the heterogeneous drop-by-drop

application of glucose when compared to the well-mixed, homogeneous application of the substrate. This effect of spatial heterogeneity can in large part be attributed to nutrient limitation: in the heterogeneous treatment, the local availability of nutrients in the substrate hotspots was not sufficient to sustain the high microbial growth rate in the presence of a large excess of C. On the other hand, mixing alleviated this limitation by distributing the same amount of glucose more evenly across the sample, such that sufficient soil-derived nutrients were available. This is plausible given that the soil used was sampled from an experimental site with long-term fertilization with farmyard manure (Holthusen et al., 2012; Seidel et al., 2021, Table S1 soil characteristics) and because the addition of a full nutrient solution instead of just glucose did not yield any discernible difference in the dynamics of the homogenized treatments (Fig. 2). This indicates no general nutrient limitation in this soil, although such limitations are commonly found in respiration experiments with many diverse soils (e.g., Sawada et al., 2017).

However, the fact that the dropwise heterogeneous addition of glucose was sufficient to induce local nutrient limitation in this soil highlights the need for careful consideration of both (i) experimental protocols and (ii) microbial dynamics in natural soils, where substrate (and nutrient) availability is highly localized in space and time (Kuzuyakov and Blagodatskaya, 2015). Notably, we only used a single rate of glucose addition (1 mg glucose/g soil, corresponding to ~2.5 MBC) across treatments in this experiment. According to our results, we would predict that adding larger amounts of C should begin to induce a similar nutrient limitation even in homogenized samples, as the (equally distributed) glucose concentration approaches the one experienced locally by microbes in our heterogeneous incubations. Conversely, lower rates of C addition should alleviate the nutrient limitation even in heterogeneous treatments. The rate of glucose addition is well known to strongly affect the outcome of respiration experiments (e.g., Schneck-enberger et al., 2008; Reischke et al., 2014; Rousk et al., 2014), and varying it would thus be an option to investigate the details of the induced nutrient limitation and its role in determining the effect of substrate spatial heterogeneity (see also Iltstedt et al., 2006; Gnankam-bary et al., 2008). In particular, functional differences in microbial communities may only affect soil C dynamics under conditions that do not constrain microbial activity (Nunan et al., 2017).

A similar pattern of reduced maximum heat release rates and prolonged heat production after glucose addition in soil microcosms with varying degrees of substrate spatial heterogeneity has previously been explained by the possible effects of substrate diffusion and the co-location of substrate and microorganisms (Shi et al., 2021). The importance of such effects has long been studied both empirically and via modelling across scales (e.g., Gaillard et al., 1999; Portell et al., 2018), yet they cannot explain the strongly reduced effect of substrate spatial availability in our experiment in the presence of additional nutrients (critically, no nutrients were added along with glucose in the experiment of Shi et al., 2021). Nonetheless, we do still find a small delay and reduction in the activity of the heterogeneous treatment after nutrient addition (Fig. 2b–d), which we assume to be caused by such a consumer-resource dislocation as discussed in Shi et al. (2021). Specifically, even if nutrients are sufficient, the exponential growth of microbes exposed to substrate in a smaller number of hotspots lagged behind that of samples in which all microbes had immediate access to the evenly distributed substrate (Fig. 2b–d).

The dynamics of CO<sub>2</sub> and heat release of all treatments were adequately captured by the simple model of aerobic microbial growth on glucose and an additional nutrient pool, representing a nutrient proxy comprising all essential nutrients. Specifically, the elevated rates of CO<sub>2</sub> and heat release well beyond the respective peaks in the heterogeneous treatment in Fig. 2a–c can be explained by the continued consumption of glucose by microbes in the model, which are unable to make use of all of the available substrate during the exponential growth phase due to nutrient limitation. Instead, they continue to grow for a longer period

and reach a similar biomass by the time all available glucose has been consumed (Fig. S3b), even though they cannot grow as quickly under the nutrient-limited conditions early in the incubation. This intuition is supported by very similar overall CUE (and EUE) in the model after 50 h across treatments (Fig. 4a).

Importantly, the model did not include any spatially explicit structure, and a minimal representation of nutrient availability via Michaelis-Menten-type kinetics was sufficient to quantitatively capture the patterns in the observed data (Fig. 2). Effectively, the low nutrient concentrations (corresponding to the limited amount available in substrate hotspots) acted to lower the overall microbial growth rate, an effect that was studied in detail by Chakrawal et al. (2022). Intriguingly, the model calibration also accounted for the substrate spatial heterogeneity by reducing overall microbial activity in heterogeneous treatments, regardless of nutrient status (Fig. S3c). While the initial MBC in the model was fixed to the experimentally determined value (155 µg C g<sup>-1</sup>, details in S1 Text), this behavior can be interpreted as lowering the effective initial model MBC, with a smaller part of the microbial community reacting to the constant amount of added substrate. This mimics the smaller co-location of (or larger distance between) substrate and consumers (e.g., Pinheiro et al., 2015; Babey et al., 2017) without a spatially explicit structure and accounts for the residual effect of substrate spatial heterogeneity in the absence of nutrient limitation.

While the nutrient limitation changed the temporal dynamics of microbial growth in the corresponding treatments, neither the model nor the experimental data indicated a substantial reduction in microbial growth yield after 50 h (Fig. 4a). Instead, all incubations and simulations were characterized by very similar values of CUE<sub>S</sub> and EUE<sub>S</sub> broadly in the range of 0.55–0.65 (Fig. 4a), which is consistent with theoretical constraints and empirical observations of efficient aerobic growth on glucose (e.g., Heijnen and Van Dijken, 1992; Trapp et al., 2018); Remarkably, Inagaki et al. (2023) observed a very similar pattern in a recent study, but these authors were using plant-derived organic matter as a more complex carbon source and performed longer incubations. After substrate addition either in hotspots or homogeneously to topsoil, they also found a pronounced effect of heterogeneity on the process rates but not on the efficiency based on cumulative CO<sub>2</sub>.

Although the estimation of growth based solely on CO<sub>2</sub> or heat release using CUE<sub>S</sub> and EUE<sub>S</sub> is generally problematic (Hagerty et al., 2018), both estimates were in good agreement in our experiment, and their underlying assumption of complete substrate consumption was justified after 50 h (Fig. S3a). Moreover, we found that EUE<sub>S</sub> consistently exceeded CUE<sub>S</sub>, in line with theory (S1 Text) and contrary to the recent review by Wang and Kuzuyakov (2023). However, both estimates as well as model simulations indicated a larger biomass growth than did dsDNA, although dsDNA was only measured in the homogenized treatment without nutrient addition. In part, these differences may be explained by variability in the initial biomass in our incubations (S1 Text). Yet, this observation might also indicate that not all glucose consumed is immediately used for growth with a corresponding proportional increase in dsDNA, and that the conversion factor between dsDNA and biomass carbon initially increases after substrate addition (Čapek et al., 2023, details in S1 Text). In any case, the direct quantification of MBC and especially the use of isotope-labeled substrates would greatly strengthen any future investigations.

Overall, our first hypothesis regarding microbial growth was therefore only partly confirmed. While we did observe reduced and delayed microbial activity under spatially heterogeneous conditions in the treatment without nutrient addition, this impaired activity was only partly observed when nutrients were added in parallel. Moreover, all available estimates and the dynamic model indicate that net growth was comparable among the treatments after 50 h of incubation. Finally, nutrient limitation (though not O<sub>2</sub>, see below) was indeed the more important cause behind this effect of substrate spatial heterogeneity when compared to the spatial separation of glucose and microbes, confirming the nutrient aspect of our second hypothesis.

#### 4.2. Substrate spatial heterogeneity does not induce local O<sub>2</sub> limitation

We also hypothesized that local oxygen availability might be another limiting factor for microbial growth under heterogeneous substrate conditions and could potentially induce anaerobic metabolism. Conceptually, microbial O<sub>2</sub> demand in the presence of high substrate concentrations has the potential to locally outpace physical O<sub>2</sub> supply and contribute to the formation of anoxic microsites that form on microbial hotspots. The importance of this mechanism has been recognized even in well-drained upland soils (e.g., Keiluweit et al., 2017; Lacroix et al., 2022). However, we found no evidence of substantial anaerobiosis in our experiment, with neither the direct O<sub>2</sub> measurements nor any of the cumulative ratios (CR, CR<sub>O<sub>2</sub></sub>, RQ) indicating such an O<sub>2</sub> limitation in our incubations (Figs. 2 and 3, Fig. S2). Furthermore, substantial contributions of anaerobic metabolism would leave a distinct signature in the CR depending on the specific metabolic pathway (Barros et al., 2016; Boye et al., 2018; Chakrawal et al., 2020), and any CO<sub>2</sub> produced anaerobically would elevate RQ values. In addition, any demand-driven O<sub>2</sub> limitation should arguably be at least as severe in the treatments with nutrient addition, yet we did not find substantial differences in the dynamics or microbial efficiency of those incubations. Lastly, the model was also able to accurately capture the observed dynamics assuming a purely aerobic (growth and maintenance) metabolism.

Importantly, even though the soil in the treatments simulating heterogeneous conditions was not mixed after the dropwise application of glucose, the soil used for all samples had been sieved, dried, rewetted, and mixed beforehand. Consequently, any comparison or inference to natural soils with intact structure that may promote the formation of anoxic conditions is not feasible. Similarly, the soil disturbance will disrupt the local microbial community and alter its use of the labile substrate, e.g., regarding rate and efficiency, when compared to undisturbed soil (Thomson et al., 2010; Ruamps et al., 2011).

Finally, we note that anaerobic pathways such as fermentations may also be carried out by microbes under purely aerobic conditions if substrate concentration is high, a phenomenon sometimes termed overflow metabolism (Basan et al., 2015). While this would affect the assumption of complete conversion of glucose to biomass and CO<sub>2</sub>, we suggest that it likely did not occur to a significant extent in our experiment, since the measured cumulative ratios (Fig. 3) did not reveal any pattern characteristic of these fermentations (Chakrawal et al., 2020).

#### 4.3. Leveraging coupled carbon and energy fluxes

Our estimates of the cumulative CR were consistent with efficient aerobic growth of microbes on glucose and indicated no substantial deviations, e.g., caused by anaerobiosis (Barros et al., 2016; Chakrawal et al., 2020). In essence, both the carbon and energy balances suggest a similar, simple interpretation of our experimental findings (Figs. 3 and 4). CR should be understood as the ratio of the corresponding (instantaneous) rates of CO<sub>2</sub> and heat production, and thus as a dynamic quantity (Hansen et al., 2004). In fact, the use of total cumulative values for the CR calculation is equivalent to using the average production rates over the incubation, thereby muting any temporal pattern. While such a simplification has been used before (e.g., Herrmann and Bölscher, 2015), it greatly reduces the amount of available information, and we found pronounced temporal variation of the CR in all treatments (Fig. 5, Fig. S4). Hence, the full potential of the framework could be leveraged by including this dynamic information in the analysis.

For example, the consistent shift from higher CR values during the exponential growth phase to lower values after the onset of the retardation phase when substrate is depleted (Fig. S4) was also recently observed in a similar experiment using the same soil (Yang et al., 2024) and may be interpreted as a shift from growth metabolism to a metabolism dominated by maintenance processes. When using cumulative CR, averaging the rates across the exponential and retardation phases would mask the individual CR values of these processes and alter the

relationship between observed CUE and (cumulative) CR. This may also account for some of the observed deviation from theoretical predictions in Fig. 4B, which are based on pure growth without maintenance (for details, see also S1 Text).

In contrast, the shift in dynamic CR is mechanistically captured by the dynamic model via a decrease in the active fraction of biomass (Fig. S3c) and a transition from exogenous (glucose-consuming) to endogenous (biomass carbon-consuming) maintenance (Wang and Post, 2012) once the substrate is depleted (Fig. S4). Nonetheless, based on heat and CO<sub>2</sub> alone, the model cannot distinguish between different equally plausible (biochemical) processes that could result in the specific lower CR value during the retardation phase, e.g., the use of SOM, necromass formation, or consumption of storage compounds (details S1 Text). This conceptual limitation of the CR, which integrates the contributions of all heat- and CO<sub>2</sub>-producing processes, could at least in part be overcome by additional measurements, in particular by monitoring biomass (composition) and by using labeled substrates. Such measurements would also help to improve parameter identifiability, which is often low in soil biogeochemical models like the one employed here (see e.g. Sierra et al., 2015; Marschmann et al., 2019). Specifically, observations of these additional carbon pools can reduce equifinality, the phenomenon that multiple (complex) model formulations and parameterizations yield identical dynamics of the (limited) observed data, which remains a major challenge (Wieder et al., 2015).

The quantitative interpretation of dynamic CR curves also faces substantial challenges from an experimental perspective. One source of error stems from the fact that the (dynamic) CR is highly sensitive to even minor shifts in the relative timing of CO<sub>2</sub> and heat, due to its nature as a quotient. In particular, the measurement of CO<sub>2</sub> and heat in separate incubations, which frequently also takes place in different types of vessels, requires matching experimental conditions (e.g., keeping the same soil-to-head space volume as in our study) to minimize potential effects on CR dynamics. This problem has been recognized, but the development of setups allowing the simultaneous measurement of CO<sub>2</sub> and heat is still ongoing (Barros et al., 2010; Yang et al., 2024).

Our modified model variant (Fig. 5a), in which CO<sub>2</sub> is measured after an additional transport process mimicking the diffusion of the gas from its site of production (microbes in the soil) to the site of detection (alkali solution above the headspace), illustrates this problem. The transport causes a relative delay of CO<sub>2</sub> compared to heat of around 1.2–1.8h, which is consistent with simple estimates of the diffusion time in our experimental system (Fig. 5b, details are presented in S1 Text). Intriguingly, this moderate shift in timing induced an artificial temporal CR pattern in the model which resembles those observed in our treatments (Fig. 5c) as well as in the literature (e.g., Barros et al., 2010). Thus, the quantitative evaluation of the dynamic CR requires a careful disentanglement of features that may be caused by the experimental setup from those corresponding to actual microbial activity, such as a slightly faster (0.5–2 h) heat vs CO<sub>2</sub> release in response to the input of labile substrate. While this is beyond the scope and data availability of this study, future work aiming at simultaneous measurements of carbon and energy fluxes would benefit from the use of labeled substrates to quantify potential biases. This will enable the full utilization of this promising tool to obtain a mechanistic, bioenergetic understanding of the soil system.

#### 4.4. Conclusion

Based on rates of CO<sub>2</sub> and heat production, substrate spatial heterogeneity resulted in reduced but prolonged microbial activity in glucose-amended soil. This effect could be attributed to local nutrient limitation and was mitigated if nutrients were added along with glucose, while we found no evidence of substantial oxygen limitation in any of our incubations. The observed dynamics were well described by a simple model of aerobic microbial growth. Notably, both simulations and experimental evidence revealed no significant effect of spatial



heterogeneity or nutrient addition on the overall CUE and EUE after 50 h. These findings demonstrate that local nutrient availability in soils can be the major factor limiting microbial growth rates, but not necessarily efficiency, if C sources have patchy distributions in space and time. Conversely, microbes in substrate hotspots may be able to compensate for the smaller overall co-location of consumers and substrate in the soil if ample nutrients are available in those hotspots.

Furthermore, the joint application experimental and process-based modeling techniques is a powerful tool for the analysis of microbial dynamics in soil. In this study, data-model integration provided mechanistic insights on the contributions of nutrient limitation and reduced microbial activity to the observed effect of substrate spatial heterogeneity, and quantitatively revealed potential biases arising from the combination of temporal CO<sub>2</sub> and heat measurements. If such artifacts are accounted for, future analyses may harness the full potential of this bioenergetic framework to study the dynamics of coupled C- and energy fluxes in the soil system.

Finally, our observations also illustrate that even relatively minor differences in the application of labile substrate to soils, like (lack of) thorough mixing after glucose amendment, do not affect the overall CUE and EUE values, but they have the potential to significantly alter the dynamics in a laboratory setting. The possibility of such methodological details introducing artificial patterns must be carefully evaluated in the specific context of similar experiments.

#### CRediT authorship contribution statement

**Martin-Georg Endress:** Writing – review & editing, Writing – original draft, Visualization, Software, Formal analysis, Data curation. **Fatemeh Dehghani:** Writing – review & editing, Writing – original draft, Visualization, Validation, Investigation, Data curation. **Sergey Blagodatsky:** Writing – review & editing, Supervision, Project administration, Methodology, Funding acquisition, Conceptualization. **Thomas Reitz:** Writing – review & editing, Supervision, Project administration, Methodology, Funding acquisition, Conceptualization. **Steffen Schlüter:** Writing – review & editing, Supervision, Project administration, Methodology, Funding acquisition, Conceptualization. **Evgenia Blagodatskaya:** Writing – review & editing, Supervision, Project administration, Methodology, Funding acquisition, Conceptualization.

#### Declaration of competing interest

The authors declare the following financial interests/personal relationships which may be considered as potential competing interests:

All authors report that financial support was provided by the German Research Foundation. All authors declare that they have no other known competing financial interests or personal relationships that could have appeared to influence the work reported in this paper.

#### Data availability

All data analyzed during this study are included in this published article and its supplementary files. All modeling code is available from the corresponding author upon reasonable request.

#### Acknowledgments

This study was performed within the framework of the German Science Foundation (DFG) Priority Program “SPP 2322 – System ecology of soils – Energy Discharge Modulated by Microbiome and Boundary Conditions (SoilSystems)”. The work was funded by the DFG under the grants 465124939 (MGE, SB) and 465122443 (FD, TR, SS, EB). Schematics (Figs. 1 and 5a) were created with BioRender.

#### Appendix A. Supplementary data

Supplementary data to this article can be found online at <https://doi.org/10.1016/j.soilbio.2024.109509>.

#### References

- Babey, T., Vieublé-Gonod, L., Rapaport, A., Pinheiro, M., Garnier, P., De Dreuzy, J.-R., 2017. Spatiotemporal simulations of 2,4-D pesticide degradation by microorganisms in 3D soil-core experiments. *Ecological Modelling* 344, 48–61. <https://doi.org/10.1016/j.ecolmodel.2016.11.006>.
- Bajracharya, B.M., Smeaton, C.M., Markelov, I., Markelova, E., Lu, C., Cirkpa, O.A., Cappellen, P.V., 2022. Organic-matter degradation in energy-limited subsurface environments—a bioenergetics-informed modeling approach. *Geomicrobiology Journal* 39, 1–16. <https://doi.org/10.1080/01490451.2021.1998256>.
- Bardgett, R.D., Freeman, C., Ostle, N.J., 2008. Microbial contributions to climate change through carbon cycle feedbacks. *The ISME Journal* 2, 805–814. <https://doi.org/10.1038/ismej.2008.58>.
- Barros, N., Hansen, L.D., Piñero, V., Pérez-Cruzado, C., Villanueva, M., Proupín, J., Rodríguez-Anón, J.A., 2016. Factors influencing the calorespirometric ratios of soil microbial metabolism. *Soil Biology and Biochemistry* 92, 221–229. <https://doi.org/10.1016/j.soilbio.2015.10.007>.
- Barros, N., Salgado, J., Rodríguez-Anón, J.A., Proupín, J., Villanueva, M., Hansen, L.D., 2010. Calorimetric approach to metabolic carbon conversion efficiency in soils: comparison of experimental and theoretical models. *Journal of Thermal Analysis and Calorimetry* 99, 771–777. <https://doi.org/10.1007/s10973-010-0673-4>.
- Basan, M., Hui, S., Okano, H., Zhang, Z., Shen, Y., Williamson, J.R., Hwa, T., 2015. Overflow metabolism in *Escherichia coli* results from efficient proteome allocation. *Nature* 528, 99–104. <https://doi.org/10.1038/nature15765>.
- Blagodatsky, S.A., Richter, O., 1998. Microbial growth in soil and nitrogen turnover: a theoretical model considering the activity state of microorganisms. *Soil Biology and Biochemistry* 30, 1743–1755. [https://doi.org/10.1016/S0038-0717\(98\)00028-5](https://doi.org/10.1016/S0038-0717(98)00028-5).
- Boye, K., Herrmann, A.M., Schaefer, M.V., Tfaily, M.M., Fendorf, S., 2018. Discerning microbially mediated processes during redox transitions in flooded soils using carbon and energy balances. *Frontiers in Environmental Science* 6, 15. <https://doi.org/10.3389/fenvs.2018.00015>.
- Čapek, P., Choma, M., Kaštovská, E., Tahovská, K., Glanville, H.C., Šantrůčková, H., 2023. Revisiting soil microbial biomass: considering changes in composition with growth rate. *Soil Biology and Biochemistry* 184, 109103. <https://doi.org/10.1016/j.soilbio.2023.109103>.
- Chakrawal, A., Calabrese, S., Herrmann, A.M., Manzoni, S., 2022. Interacting bioenergetic and stoichiometric controls on microbial growth. *Frontiers in Microbiology* 13, 859063. <https://doi.org/10.3389/fmicb.2022.859063>.
- Chakrawal, A., Herrmann, A.M., Manzoni, S., 2021. Leveraging energy flows to quantify microbial traits in soils. *Soil Biology and Biochemistry* 155, 108169. <https://doi.org/10.1016/j.soilbio.2021.108169>.
- Chakrawal, A., Herrmann, A.M., Šantrůčková, H., Manzoni, S., 2020. Quantifying microbial metabolism in soils using calorespirometry — a bioenergetics perspective. *Soil Biology and Biochemistry* 148, 107945. <https://doi.org/10.1016/j.soilbio.2020.107945>.
- Chapman, S.B., 1971. A simple conductimetric soil respirometer for field use. *Oikos* 22, 348–353. <https://doi.org/10.2307/3543857>.
- Chen, R., Senbayram, M., Blagodatsky, S., Myachina, O., Dittert, K., Lin, X., Blagodatskaya, E., Kuzyakov, Y., 2014. Soil C and N availability determine the priming effect: microbial N mining and stoichiometric decomposition theories. *Global Change Biology* 20, 2356–2367. <https://doi.org/10.1111/gcb.12475>.
- Coppens, F., Merckx, R., Recous, S., 2006. Impact of crop residue location on carbon and nitrogen distribution in soil and in water-stable aggregates. *European Journal of Soil Science* 57, 570–582. <https://doi.org/10.1111/j.1365-2389.2006.00825.x>.
- Crowther, T.W., Van Den Hoogen, J., Wan, J., Mayes, M.A., Keiser, A.D., Mo, L., Averill, C., Maynard, D.S., 2019. The global soil community and its influence on biogeochemistry. *Science* 365, eaav0550. <https://doi.org/10.1126/science.aav0550>.
- Dungait, J.A.J., Hopkins, D.W., Gregory, A.S., Whitmore, A.P., 2012. Soil organic matter turnover is governed by accessibility not recalcitrance. *Global Change Biology* 18, 1781–1796. <https://doi.org/10.1111/j.1365-2486.2012.02665.x>.
- Endress, M.-G., Chen, R., Blagodatskaya, E., Blagodatsky, S., 2024. The coupling of carbon and energy fluxes reveals anaerobiosis in an aerobic soil incubation with a *Bacillota*-dominated community. *Soil Biology and Biochemistry* 195, 109478. <https://doi.org/10.1016/j.soilbio.2024.109478>.
- Gaillard, V., Chenu, C., Recous, S., Richard, G., 1999. Carbon, nitrogen and microbial gradients induced by plant residues decomposing in soil. *European Journal of Soil Science* 50, 567–578. <https://doi.org/10.1046/j.1365-2389.1999.00266.x>.
- Geyer, K.M., Kyker-Snowman, E., Grandy, A.S., Frey, S.D., 2016. Microbial carbon use efficiency: accounting for population, community, and ecosystem-scale controls over the fate of metabolized organic matter. *Biogeochemistry* 127, 173–188. <https://doi.org/10.1007/s10533-016-0191-y>.
- Gnankambary, Z., Ilstedt, U., Nyberg, G., Hien, V., Malmer, A., 2008. Nitrogen and phosphorus limitation of soil microbial respiration in two tropical agroforestry parklands in the south-Sudanese zone of Burkina Faso: the effects of tree canopy and fertilization. *Soil Biology and Biochemistry* 40, 350–359. <https://doi.org/10.1016/j.soilbio.2007.08.015>.
- Gunina, A., Kuzyakov, Y., 2022. From energy to (soil organic) matter. *Global Change Biology* 28, 2169–2182. <https://doi.org/10.1111/gcb.16071>.

- Hagerty, S.B., Allison, S.D., Schimel, J.P., 2018. Evaluating soil microbial carbon use efficiency explicitly as a function of cellular processes: implications for measurements and models. *Biogeochemistry* 140, 269–283. <https://doi.org/10.1007/s10533-018-0489-z>.
- Hansen, L.D., Macfarlane, C., McKinnon, N., Smith, B.N., Criddle, R.S., 2004. Use of calorespirometric ratios, heat per CO<sub>2</sub> and heat per O<sub>2</sub>, to quantify metabolic paths and energetics of growing cells. *Thermochimica Acta* 422, 55–61. <https://doi.org/10.1016/j.tca.2004.05.033>.
- Heijnen, J.J., Van Dijken, J.P., 1992. In search of a thermodynamic description of biomass yields for the chemotrophic growth of microorganisms. *Biotechnology and Bioengineering* 39, 833–858. <https://doi.org/10.1002/bit.260390806>.
- Herrmann, A.M., Bölscher, T., 2015. Simultaneous screening of microbial energetics and CO<sub>2</sub> respiration in soil samples from different ecosystems. *Soil Biology and Biochemistry* 83, 88–92. <https://doi.org/10.1016/j.soilbio.2015.01.020>.
- Holthausen, D., Jänicke, M., Peth, S., Horn, R., 2012. Physical properties of a Luvisol for different long-term fertilization treatments: I. Mesoscale capacity and intensity parameters. *Journal of Plant Nutrition and Soil Science* 175, 4–13. <https://doi.org/10.1002/jpln.201100075>.
- Ilstedt, U., Nordgren, A., Malmer, A., 2006. Soil chemical and microbial properties after disturbance by crawler tractors in a Malaysian forest plantation. *Forest Ecology and Management* 225, 313–319. <https://doi.org/10.1016/j.foreco.2006.01.008>.
- Inagaki, T.M., Possinger, A.R., Schweizer, S.A., Mueller, C.W., Hoeschen, C., Zachman, M.J., Kourkoutis, L.F., Kögel-Knabner, I., Lehmann, J., 2023. Microscale spatial distribution and soil organic matter persistence in top and subsoil. *Soil Biology and Biochemistry* 178, 108921. <https://doi.org/10.1016/j.soilbio.2022.108921>.
- Juarez, S., Nunan, N., Duda, A.-C., Pouteau, V., Schmidt, S., Falconer, R., Otten, W., Chenu, C., 2013. Effects of different soil structures on the decomposition of native and added organic carbon. *European Journal of Soil Biology* 58, 81–90. <https://doi.org/10.1016/j.ejsobi.2013.06.005>.
- Kandeler, E., 1999. Xylanase, invertase and protease at the soil–litter interface of a loamy sand. *Soil Biology and Biochemistry* 31, 1171–1179. [https://doi.org/10.1016/S0038-0717\(99\)00035-8](https://doi.org/10.1016/S0038-0717(99)00035-8).
- Keilueit, M., Wanzek, T., Kleber, M., Nico, P., Fendorf, S., 2017. Anaerobic microsites have an unaccounted role in soil carbon stabilization. *Nature Communications* 8, 1771. <https://doi.org/10.1038/s41467-017-01406-6>.
- Kim, K., Kutlu, T., Kravchenko, A., Guber, A., 2021. Dynamics of N<sub>2</sub>O in vicinity of plant residues: a microsensor approach. *Plant and Soil* 462, 331–347. <https://doi.org/10.1007/s11104-021-04871-7>.
- Korsaeht, A., Molstad, L., Bakken, L.R., 2001. Modelling the competition for nitrogen between plants and micro-ora as a function of soil heterogeneity. *Soil Biology*.
- Kuka, K., Franko, U., Rühlmann, J., 2007. Modelling the impact of pore space distribution on carbon turnover. *Ecological Modelling* 208, 295–306. <https://doi.org/10.1016/j.ecolmodel.2007.06.002>.
- Kuzyakov, Y., Blagodatskaya, E., 2015. Microbial hotspots and hot moments in soil: concept & review. *Soil Biology and Biochemistry* 83, 184–199. <https://doi.org/10.1016/j.soilbio.2015.01.025>.
- Lacroix, E.M., Aeppli, M., Boye, K., Brodie, E., Fendorf, S., Keilueit, M., Naughton, H.R., Noël, V., Sibi, D., 2023. Consider the anoxic microsite: acknowledging and appreciating spatiotemporal redox heterogeneity in soils and sediments. *ACS Earth and Space Chemistry* 7, 1592–1609. <https://doi.org/10.1021/acsearthspacechem.3c00032>.
- Lacroix, E.M., Mendillo, J., Gomes, A., Dekas, A., Fendorf, S., 2022. Contributions of anoxic microsites to soil carbon protection across soil textures. *Geoderma* 425, 116050. <https://doi.org/10.1016/j.geoderma.2022.116050>.
- Lehmann, J., Hansel, C.M., Kaiser, C., Kleber, M., Maher, K., Manzoni, S., Nunan, N., Reichstein, M., Schimel, J.P., Torn, M.S., Wieder, W.R., Kögel-Knabner, I., 2020. Persistence of soil organic carbon caused by functional complexity. *Nature Geoscience* 13, 529–534. <https://doi.org/10.1038/s41561-020-0612-3>.
- Lenth, R.V., 2023. *Emmeans: Estimated Marginal Means, Aka Least-Squares Means*.
- Loecke, T.D., Robertson, G.P., 2009. Soil resource heterogeneity in terms of litter aggregation promotes nitrous oxide fluxes and slows decomposition. *Soil Biology and Biochemistry* 41, 228–235. <https://doi.org/10.1016/j.soilbio.2008.10.017>.
- Magid, J., De Neergaard, A., Brandt, M., 2006. Heterogeneous distribution may substantially decrease initial decomposition, long-term microbial growth and N-immobilization from high C-to-N ratio resources. *European Journal of Soil Science* 57, 517–529. <https://doi.org/10.1111/j.1365-2389.2006.00805.x>.
- Manzoni, S., 2017. Flexible carbon-use efficiency across litter types and during decomposition partly compensates nutrient imbalances—results from analytical stoichiometric models. *Frontiers in Microbiology* 8.
- Manzoni, S., Capek, P., Porada, P., Thurner, M., Winterdahl, M., Beer, C., Brüchert, V., Frouz, J., Herrmann, A.M., Lindahl, B.D., Lyon, S.W., Šantrůčková, H., Vico, G., Way, D., 2018. Reviews and syntheses: carbon use efficiency from organisms to ecosystems – definitions, theories, and empirical evidence. *Biogeosciences* 15, 5929–5949. <https://doi.org/10.5194/bg-15-5929-2018>.
- Manzoni, S., Taylor, P., Richter, A., Porporato, A., Ågren, G.I., 2012. Environmental and stoichiometric controls on microbial carbon-use efficiency in soils. *New Phytologist* 196, 79–91.
- Marschmann, G.L., Pagel, H., Kügler, P., Streck, T., 2019. Equifinality, sloppiness, and emergent structures of mechanistic soil biogeochemical models. *Environmental Modelling & Software* 122, 104518. <https://doi.org/10.1016/j.envsoft.2019.104518>.
- Moyano, F.E., Manzoni, S., Chenu, C., 2013. Responses of soil heterotrophic respiration to moisture availability: an exploration of processes and models. *Soil Biology and Biochemistry* 59, 72–85. <https://doi.org/10.1016/j.soilbio.2013.01.002>.
- Newville, M., Otten, R., Nelson, A., Stensitzki, T., Ingargiola, A., Allan, D., Fox, A., Carter, F., Michal, Osborn, R., Pustakhod, D., Ineuhaus, Weigand, S., Aristov, A., Glenn, Deil, C., mgunyo, Mark, Hansen, A.L.R., Pasquevich, G., Foks, L., Zobrist, N., Frost, O., Stuermer, azelcer, Polloreno, A., Persaud, A., Nielsen, J.H., Pompili, M., Eendebak, P., 2023. Lmfit/Lmfit-Py: 1.2.2. <https://doi.org/10.5281/zenodo.8145703>.
- Nordgren, A., 1988. Apparatus for the continuous, long-term monitoring of soil respiration rate in large numbers of samples. *Soil Biology and Biochemistry* 20, 955–957. [https://doi.org/10.1016/0038-0717\(88\)90110-1](https://doi.org/10.1016/0038-0717(88)90110-1).
- Nunan, N., 2017. The microbial habitat in soil: scale, heterogeneity and functional consequences. *Journal of Plant Nutrition and Soil Science* 180, 425–429. <https://doi.org/10.1002/jpln.201700184>.
- Nunan, N., Leloup, J., Ruamps, L.S., Pouteau, V., Chenu, C., 2017. Effects of habitat constraints on soil microbial community function. *Scientific Reports* 7, 4280. <https://doi.org/10.1038/s41598-017-04485-z>.
- Nunan, N., Schmidt, H., Raynaud, X., 2020. The ecology of heterogeneity: soil bacterial communities and C dynamics. *Philosophical Transactions of the Royal Society B: Biological Sciences* 375, 20190249. <https://doi.org/10.1098/rstb.2019.0249>.
- Or, D., Smets, B.F., Wraith, J.M., Dechesne, A., Friedman, S.P., 2007. Physical constraints affecting bacterial habitats and activity in unsaturated porous media – a review. *Advances in Water Resources* 30, 1505–1527. <https://doi.org/10.1016/j.advwatres.2006.05.025>.
- Panikov, N.S., 1996. Mechanistic mathematical models of microbial growth in bioreactors and in natural soils: explanation of complex phenomena. *Mathematics and Computers in Simulation* 42, 179–186. [https://doi.org/10.1016/0378-4754\(95\)00127-1](https://doi.org/10.1016/0378-4754(95)00127-1).
- Peth, S., Chenu, C., Leblond, N., Mordhorst, A., Garnier, P., Nunan, N., Pot, V., Ogurek, M., Beckmann, F., 2014. Localization of soil organic matter in soil aggregates using synchrotron-based X-ray microtomography. *Soil Biology and Biochemistry* 78, 189–194. <https://doi.org/10.1016/j.soilbio.2014.07.024>.
- Phillips, C., Nickerson, N., 2015. *Soil Respiration*.
- Pinheiro, M., Garnier, P., Beguet, J., Martin Laurent, F., Vieublé Gonod, L., 2015. The millimeter-scale distribution of 2,4-D and its degraders drives the fate of 2,4-D at the soil core scale. *Soil Biology and Biochemistry* 88, 90–100. <https://doi.org/10.1016/j.soilbio.2015.05.008>.
- Poll, C., Ingwersen, J., Stemmer, M., Gerzabek, M.H., Kandeler, E., 2006. Mechanisms of solute transport affect small-scale abundance and function of soil microorganisms in the detritusphere. *European Journal of Soil Science* 57, 583–595. <https://doi.org/10.1111/j.1365-2389.2006.00835.x>.
- Portell, X., Pot, V., Garnier, P., Otten, W., Baveye, P.C., 2018. Microscale heterogeneity of the spatial distribution of organic matter can promote bacterial biodiversity in soils: insights from computer simulations. *Frontiers in Microbiology* 9, 1583. <https://doi.org/10.3389/fmicb.2018.01583>.
- R Core Team, 2023. *R: A Language and Environment for Statistical Computing*. R Foundation for Statistical Computing, Vienna, Austria.
- Raynaud, X., Nunan, N., 2014. Spatial ecology of bacteria at the microscale in soil. *PLoS One* 9, e87217. <https://doi.org/10.1371/journal.pone.0087217>.
- Reischke, S., Rousk, J., Bååth, E., 2014. The effects of glucose loading rates on bacterial and fungal growth in soil. *Soil Biology and Biochemistry* 70, 88–95. <https://doi.org/10.1016/j.soilbio.2013.12.011>.
- Rousk, J., Hill, P.W., Jones, D.L., 2014. Using the concentration-dependence of respiration arising from glucose addition to estimate in situ concentrations of labile carbon in grassland soil. *Soil Biology and Biochemistry* 77, 81–88. <https://doi.org/10.1016/j.soilbio.2014.06.015>.
- Ruamps, L.S., Nunan, N., Chenu, C., 2011. Microbial biogeography at the soil pore scale. *Soil Biology and Biochemistry* 43, 280–286. <https://doi.org/10.1016/j.soilbio.2010.10.010>.
- Russell, J.B., Cook, G.M., 1995. *Energetics of bacterial growth: balance of anabolic and catabolic reactions*. *Microbiological Reviews* 59.
- Sawada, K., Inagaki, Y., Toyota, K., Kosaki, T., Funakawa, S., 2017. Substrate-induced respiration responses to nitrogen and/or phosphorus additions in soils from different climatic and land use conditions. *European Journal of Soil Biology* 83, 27–33. <https://doi.org/10.1016/j.ejsobi.2017.10.002>.
- Schlüter, S., Leuther, F., Albrecht, L., Hoeschen, C., Kilian, R., Surey, R., Mikutta, R., Kaiser, K., Mueller, C.W., Vogel, H.-J., 2022. Microscale carbon distribution around pores and particulate organic matter varies with soil moisture regime. *Nature Communications* 13, 2098. <https://doi.org/10.1038/s41467-022-29605-w>.
- Schlüter, S., Zawallich, J., Vogel, H.-J., Dörsch, P., 2019. Physical constraints for respiration in microbial hotspots in soil and their importance for denitrification. *Biogeosciences* 16, 3665–3678. <https://doi.org/10.5194/bg-16-3665-2019>.
- Schneckenberger, K., Demin, D., Stahr, K., Kuzyakov, Y., 2008. Microbial utilization and mineralization of [14C]glucose added in six orders of concentration to soil. *Soil Biology and Biochemistry* 40, 1981–1988. <https://doi.org/10.1016/j.soilbio.2008.02.020>.
- Seidel, S.J., Gaiser, T., Ahrends, H.E., Hüging, H., Siebert, S., Bauke, S.L., Gocke, M.L., Koch, M., Schweitzer, K., Schaaf, G., Ewert, F., 2021. Crop response to P fertilizer omission under a changing climate - experimental and modeling results over 115 years of a long-term fertilizer experiment. *Field Crops Research* 268, 108174. <https://doi.org/10.1016/j.fcr.2021.108174>.
- Shi, A., Chakraval, A., Manzoni, S., Fischer, B.M.C., Nunan, N., Herrmann, A.M., 2021. Substrate spatial heterogeneity reduces soil microbial activity. *Soil Biology and Biochemistry* 152, 108068. <https://doi.org/10.1016/j.soilbio.2020.108068>.
- Sierra, C.A., Malghani, S., Müller, M., 2015. Model structure and parameter identification of soil organic matter models. *Soil Biology and Biochemistry* 90, 197–203. <https://doi.org/10.1016/j.soilbio.2015.08.012>.

- Sinsabaugh, R.L., Manzoni, S., Moorhead, D.L., Richter, A., 2013. Carbon use efficiency of microbial communities: stoichiometry, methodology and modelling. *Ecology Letters* 16, 930–939. <https://doi.org/10.1111/ele.12113>.
- Strong, D.T., Wever, H.D., Merckx, R., Recous, S., 2004. Spatial location of carbon decomposition in the soil pore system. *European Journal of Soil Science* 55, 739–750. <https://doi.org/10.1111/j.1365-2389.2004.00639.x>.
- Thomson, B.C., Ostle, N.J., McNamara, N.P., Whiteley, A.S., Griffiths, R.I., 2010. Effects of sieving, drying and rewetting upon soil bacterial community structure and respiration rates. *Journal of Microbiological Methods* 83, 69–73. <https://doi.org/10.1016/j.mimet.2010.07.021>.
- Tian, J., Pausch, J., Yu, G., Blagodatskaya, E., Gao, Y., Kuzyakov, Y., 2015. Aggregate size and their disruption affect <sup>14</sup>C-labeled glucose mineralization and priming effect. *Applied Soil Ecology* 90, 1–10. <https://doi.org/10.1016/j.apsoil.2015.01.014>.
- Trapp, S., Brock, A.L., Nowak, K., Kästner, M., 2018. Prediction of the formation of biogenic nonextractable residues during degradation of environmental chemicals from biomass yields. *Environmental Science & Technology* 52, 663–672. <https://doi.org/10.1021/acs.est.7b04275>.
- van den Broek, E., 2012. In: Good, P.I. (Ed.), *A Practitioner's Guide to Resampling for Data Analysis, Data Mining, and Modeling*. Chapman & Hall/CRC, Boca Raton, FL, 2011. - ISBN 978-1-439855-50-8. *Computing Reviews* CR139920.
- Védère, C., Vieublé Gonod, L., Pouteau, V., Girardin, C., Chenu, C., 2020. Spatial and temporal evolution of detritusphere hotspots at different soil moistures. *Soil Biology and Biochemistry* 150, 107975. <https://doi.org/10.1016/j.soilbio.2020.107975>.
- Virtanen, P., Gommers, R., Oliphant, T.E., Haberland, M., Reddy, T., Cournapeau, D., Burovski, E., Peterson, P., Weckesser, W., Bright, J., van der Walt, S.J., Brett, M., Wilson, J., Millman, K.J., Mayorov, N., Nelson, A.R.J., Jones, E., Kern, R., Larson, E., Carey, C.J., Polat, I., Feng, Y., Moore, E.W., VanderPlas, J., Laxalde, D., Perktold, J., Cimrman, R., Henriksen, I., Quintero, E.A., Harris, C.R., Archibald, A.M., Ribeiro, A. H., Pedregosa, F., van Mulbregt, P., SciPy 1.0 Contributors, 2020. *SciPy 1.0: fundamental algorithms for scientific computing in Python*. *Nature Methods* 17, 261–272. <https://doi.org/10.1038/s41592-019-0686-2>.
- Wang, C., Kuzyakov, Y., 2023. Energy use efficiency of soil microorganisms: driven by carbon recycling and reduction. *Global Change Biology* gcb.16925. <https://doi.org/10.1111/gcb.16925>.
- Wang, G., Post, W.M., 2012. A theoretical reassessment of microbial maintenance and implications for microbial ecology modeling. *FEMS Microbiology Ecology* 81, 610–617. <https://doi.org/10.1111/j.1574-6941.2012.01389.x>.
- Wieder, W.R., Allison, S.D., Davidson, E.A., Georgiou, K., Hararuk, O., He, Y., Hopkins, F., Luo, Y., Smith, M.J., Sulman, B., Todd-Brown, K., Wang, Y., Xia, J., Xu, X., 2015. Explicitly representing soil microbial processes in Earth system models. *Global Biogeochemical Cycles* 29, 1782–1800. <https://doi.org/10.1002/2015GB005188>.
- Yang, S., Di Lodovico, E., Rupp, A., Harms, H., Fricke, C., Miltner, A., Kästner, M., Maskow, T., 2024. Enhancing insights: exploring the information content of calorimetric ratio in dynamic soil microbial growth processes through calorimetry. *Frontiers in Microbiology* 15, 1321059. <https://doi.org/10.3389/fmicb.2024.1321059>.
- Zech, S., Schweizer, S.A., Bucka, F.B., Ray, N., Kögel-Knabner, I., Prechtel, A., 2022. Explicit spatial modeling at the pore scale unravels the interplay of soil organic carbon storage and structure dynamics. *Global Change Biology* 28, 4589–4604. <https://doi.org/10.1111/gcb.16230>.
- Zheng, Q., Hu, Y., Zhang, S., Noll, L., Böckle, T., Richter, A., Wanek, W., 2019. Growth explains microbial carbon use efficiency across soils differing in land use and geology. *Soil Biology and Biochemistry* 128, 45–55. <https://doi.org/10.1016/j.soilbio.2018.10.006>.
- Zinn, M., Witholt, B., Egli, T., 2004. Dual nutrient limited growth: models, experimental observations, and applications. *Journal of Biotechnology* 113, 263–279. <https://doi.org/10.1016/j.jbiotec.2004.03.030>.